Behaviour of screw connections in timber-concrete composites using low strength lightweight concrete
Peer-reviewed author version

Behaviour of screw connections in timber-concrete composites using low strength lightweight concrete

Elif Appavuravther*, Bram Vandoren, Jose Henriques

CERG, Faculty of Engineering Technology, Hasselt University, Belgium

*Corresponding author email address: eliftuba.appavuravther@uhasselt.be

Abstract

In this paper, the use of low strength lightweight concrete in combination with glue-laminated timber (TLCC) is studied. Six series of push-out tests were conducted to assess the mechanical performance of the screw shear connection between these materials with a perpendicular and inclined (shear-compression) configuration with various screw diameters and lengths. The tests show that though low strength lightweight concrete is used, composite action can still be obtained. Given the equivalent Young's modulus between the concrete and the timber, a proposal is made consisting in the use of the design approach for timber-to-timber connections in order to determine the load capacity of the tested connections, contrary of what is commonly used in the literature. The comparison with experimental tests confirm the proposed approach.

Highlight

- Experimental investigation of screws perpendicular and inclined under shear loading.
- Analysing the effect of screw diameter, embedment length and angle in the timber.
- Proposal of using timber-to-timber failure prediction models for concrete with similar modulus of elasticity to timber.

Keywords

Timber-lightweight concrete composite (TLCC), Shear connection, Push-out tests, Shear-compression loading, Inclined screws

1. Introduction

Timber-concrete composite (TCC) systems have long been used for their reliability, environmentally friendly nature and structural complementarity of materials. The shear load developed within the elements produces a slip force at the materials' interface. Therefore, to guarantee the composite behaviour, it is necessary to reduce the slip between the two materials. The composite behaviour is commonly achieved using reliable shear connectors [1], where the connection stiffness plays an important role. Consequently, these connections should be: i) stiff enough to reduce or remove slip between the two materials; ii) strong enough to resist the corresponding shear forces; and iii) ductile enough to allow a redistribution of loads amongst the several connectors used in the composite member.

Current research on TCC mainly focusses on the use of normal weight concrete. The innovation in materials leading to the development of performant lightweight concrete and the continuous search for the optimisation of structural members or systems leads to introducing lightweight concrete in TCC systems [2], which can be referred to as timber lightweight concrete composites (TLCC). Practice shows that using a mortar screed is a common way to renovate existing timber beams; however, even with high strength epoxy mortar, the structure may not reach load capacity [3]. This limitation may be due to its insufficient strength capacity, even though epoxy mortar has various strength and density classes and Young's moduli [4]. On the other hand, lightweight concrete is used due to its higher strength and added structural contribution than mortar [3]. Other advantages of lightweight concrete are its lower self-weight and creep coefficient [5]. Lightweight concrete in TCC elements requires an efficient shear connection between the two materials; therefore, their interaction can maximize the composite behaviour. However, an accurate characterisation of the interaction behaviour, between lightweight concrete and timber lacks the current standards [6, 7]. In the reported experiments, the failure of timber was observed, and therefore the concrete had minor relevance in the shear connection response due to its higher stiffness. However, if a low strength lightweight concrete is used, the shear connection's response may be governed by the brittle concrete failure. In this situation, an accurate characterisation of the connection response includes the latter.

The first step towards a composite behaviour is selecting the shear connector. Many types of connectors are used in TCC [1, 8-12], for example, self-drilling screws are commonly used in timber construction, due to their availability in various sizes, their low cost and easy installation, and preferred for use in TCC systems, in particular for renovation. Research shows that as the angle between the connector and the timber grain decreases, the stiffness of the connection increases [13]. Most researchers have preferred to position inclined screws with shear-tension loading in the connection [14-18]. Even though this may be favourable in terms of load-carrying capacity and stiffness [14], application limitations or execution mistakes (as for example is the case of renovation works with deficient technical control) can lead to shear-compression loading in the connection. Du et al. introduced shear-compression failure modes for the case in which two plastic hinge formations occur in both of the materials [19].

To further exploit the behaviour of screw connectors in TCC, this paper presents an experimental and analytical work on shear connections in TCC using low strength lightweight concrete. The studied shear connections consider screws applied perpendicular and inclined (shear-compression) to the timber grain. A total of 18 short-term push-out tests are presented for characterisation of the connection behaviour. The experimental results allowed the characterization of both configurations, perpendicular and inclined shear connectors, in terms of load-slip behaviour. Subsequently, important design parameters are highlighted, such as slip modulus, load capacity and ductility, allowing a

qualitative comparison of the studied solution as presented in Section 2. Furthermore, an evaluation of the current design approach in EN 1995-1-1 and EN 1995-2 [6, 7], together with the new Technical Specification under development for TCC is discussed as presented in Section 4 [20]. Because of the use of low strength lightweight concrete, the proposed failure modes to be considered in the characterisation of the shear connection also include possible modes of failure in the concrete side. The comparison with the experimental results provided an assessment of the applied approach and deepens the understanding of the studied shear connection behaviour.

2. Analytical characterisation of the shear connection in TLCC using screw connectors
2.1. Stiffness

The current EN 1995-1-1 does not include the design of TCC members [7]. On the other hand, the current version of the EN 1995-2 [7], which is dedicated to the design of timber bridges, covers the design of TCC bridge decks. The latter standard refers to laterally loaded dowel-type fasteners covered in the first standard to characterise the dowel type shear connection between the two materials. Accordingly, the stiffness of these type of connections, identified as slip modulus (K_{ser}), is the function of the wood mean density (ρ_{mean}) and nominal connector diameter (d). When dealing with threaded screws, as in the present study, the effective diameter (d_{ef}) should be obtained from the core diameter with d = 1.1 d_{core}. Numerous researchers [11], demonstrated the accuracy of the empirical formula prescribed by the EN 1995-1-1 for the slip modulus of connectors installed perpendicular to the timber. The proposed formula from EN 1995-1-1 is given in Eq. (1) is commonly used in timber-to-timber connections [6].

$$K_{ser} = \frac{\rho_m^{1.5} d}{23} \tag{1}$$

When a shear connection (dowel-type) is realised between concrete and timber, the EN 1995-1-1 proposes to double the slip modulus obtained using Eq. (1) as the concrete layer is assumed to be stiffer, as expressed in Eq. (2) [6]. The same approach is proposed in the Technical Specification [20].

$$K_{ser,TCC} = 2\frac{\rho_m^{1.5} d}{23} \tag{2}$$

For inclined screws that are loaded under shear-compression, Tomasi et al. recommended the use of Eq. (1) for the slip modulus prediction [14]. In this paper, it is proposed to use Eq. (1) for the combination timber - low strength lightweight concrete due to the similar Young's modulus of both materials.

2.2. Load carrying capacity

The experimental push-out tests conducted within the present study consider the installation of the shear connector (screw) perpendicular and inclined to the timber grain. For the inclined configuration, the shear connection will be activated in shear-compression.

In EN 1995-1-1, possible modes of failure and correspondent design expressions for timber-to-timber and steel-to-timber connections are given [6]. These are based on the Johansen's yield theory [21], also referred to as the European yield model. For load carrying capacity calculations of TCC, EN 1995-2 [7] suggests the use of EN 1992-2 for the concrete layer [22], and EN 1995-1-1 [6] for the timber layer. In the Technical Specification [20], however, the load carrying capacity is determined based on

the Johansen's model. Though in the design of shear connections for TCC, the "concrete" side is often assumed as rigid and strong, and therefore, neglected when determining the shear connection strength. However, due to low strength lightweight concrete's mechanical properties, a complete approach is suggested here. Du et al. supported the use of the timber-to-timber connection approach to calculate the load capacity of the shear connection in TCC, if elastic-plastic concrete behaviour is considered [19]. Hence, because different possible failure mechanism has to be taken into account, the approach followed in the present study considers the combination of the mechanical behaviour preconized for steel-to-timber and timber-to-timber connections subjected to lateral loading.

The determination of the failure modes for screws installed perpendicular to the grain is clear and straightforward for timber-to-timber and timber-to-steel composites. The Johansen's model describes the behaviour of the connection up to the onset of failure which can develop without any rotation of the screw, if one side of the connection fails before the other, or with rotation without or with development of plastic hinges in the screw. In the latter case, the rope effect phenomenon takes place which contributes to the load capacity of the connection. In EN-1995-1-1, the rope effect is accounted by including two components in Eq. (3), as detailed in [23]. The latter represent the following: i) the vertical component of the axial load on the connector, $N_d \sin \theta$, (where N_d is equal to the minimum between the tension capacity of the connector N_{ten} and the withdrawal capacity F_{ax} as given in Eq. (4)). The method consists in limiting the vertical component to 25% of F_{ax} (or the % of the Johansen's model without rope effect according to the type of fastener); ii) the friction component which is developed between the two materials and proportional to the horizontal component of N_d, given by $N_d \cos \theta \mu$. Because angle θ is unknown [23], a value of 5% and 15% is used according to the mode of failure. In this paper, the horizontal component is extrapolated based on the timber-to-concrete friction coefficient (μ) of 0.62 instead of 0.25 [13]. For mode c of timber-to-timber failure modes, no modification is proposed for the rope effect because the friction component is not considered.

$$F_{v,Rk} = N_d(\sin \theta + \mu \cos \theta) + \text{Johansen's yield load}(F_{y,Rk})$$ (3)

$$N_d = \min\{N_{ten}; F_{ax}\}$$ (4)

For inclined screws, the force distribution is more complex. In such configurations, the axial forces developed in the connector and, consequently, the withdrawal capacity, are activated from the beginning of the loading. In a recent study, Du et al. studied the behaviour of shear-compression loaded screw connectors in TCC applications with normal weight normal strength concrete [18]. The authors propose analytical methods to determine the load carrying capacity of such shear connections. However, only two possible modes of failure are considered. Consequently, the present authors propose an extension of the referred analytical approach covering all possible modes of failures. The load capacity of shear connections with inclined screws, in shear-tension connections, is approached in [16, 24]. This methodology can be similarly applied to shear-compression with the particularity that the friction coefficient has to be removed, since in shear-compression the two materials are pulled in opposite directions, and consequently, the contact between these tends to be lost.

Resultantly, in Table 1 the modes of failure are identified which determine of the load capacity of the shear connections studied in the present research. Accordingly, failure modes a to f, for timber-to-timber dowel type connections with one shear plane as developed by Bejtka and Blass [16], and failure modes c, d, and e, for steel-to-timber dowel type connections with one shear plane as developed by Kavaliauskas [24], are considered for shear compression loading. The proposed equations to determine the maximum load carrying ($F_{u,i}$) are also included. Note that in the present study, the angle (α) between the axis of the screw connector and the timber grain may vary between 0° and 90° and in the

direction for which the resulting loading mechanism is shear-compression. The axial strength (F_{ax}) represents the minimum of axial capacity of the connection between the screw connector and the timber or the concrete, as given in Eq. (5). The withdrawal strength in the timber layer ($F_{ax,timber}$) is determined according to the ETA document [25], given in Eq. (6), where ρ_k is the characteristic density of the timber, d is the nominal diameter of screw, and l_2 is the embedment length of the screw in the timber layer.

$$F_{ax} = \min\{F_{ax,timber}; F_{ax,concrete}\} \tag{5}$$

$$F_{ax,timber} = \frac{F_{ax}dl_2}{1.2\cos^2\alpha + \sin^2\alpha}\left(\frac{\rho_k}{350}\right)^{0.8} \tag{6}$$

In order to take into account the limitation of the withdrawal capacity by pull-through of the screw on the concrete side, the approach for headed anchors given in EN 1992-4 was used [26]. Due to the differences in the shape between the anchors covered in EN 1992-4 and the screws used in the current experimental programme, this approach might have a limited accuracy. Nevertheless, in the absence of a better approach, this still should provide a reliable estimation. Accordingly, the headed fastener characteristic resistance, $N_{Rk,p}$, is determined as given in Eq. (7):

$$N_{Rk,p} = k_2 A_h f_{ck} \tag{7}$$

where k_2 takes into account the uncracked (k_2 = 10.5) or cracked (k_2 = 7.5) state of the concrete (here it was assumed as uncracked); A_h is the load bearing area of head fastener; and f_{ck} is the cylinder compressive strength of the concrete. For the withdrawal capacity of concrete, $F_{ax,concrete}$, the headed fastener characteristic resistance, $N_{Rk,p}$ is used.
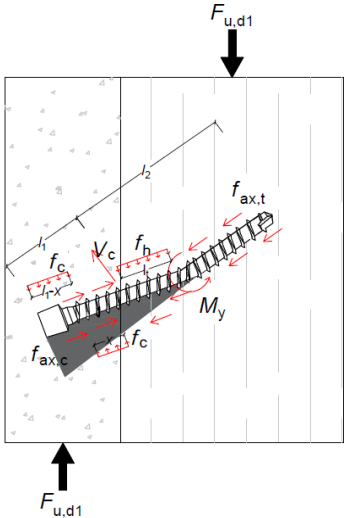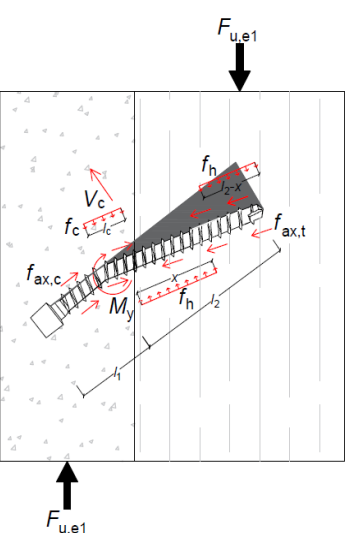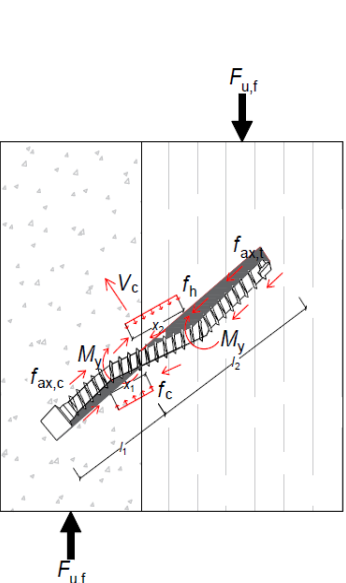
In the case of failure modes considering concrete crushing, the shear strength component is determined using the embedment strength of concrete capacity (f_c). According to the Technical Specifications it may be determined as expressed in Eq. (8) [20]. In the case when the bearing capacity of timber is reached, the embedment strength (f_h) is used and determined as given in EN 1995-1-1 [6]. Similarly, as for timber-to-timber connections, a factor β (f_h/f_c) is used. Then, for failure modes including plastic hinges in the screw connector, the yield bending strength (M_y) is incorporated in the equation. It can be determined based according to the technical specification of the connector or to EN 1995-1-1 [6]. Finally, the load bearing capacity of the connection is then governed by the weakest of the described modes of failures as expressed in Eq. (9).
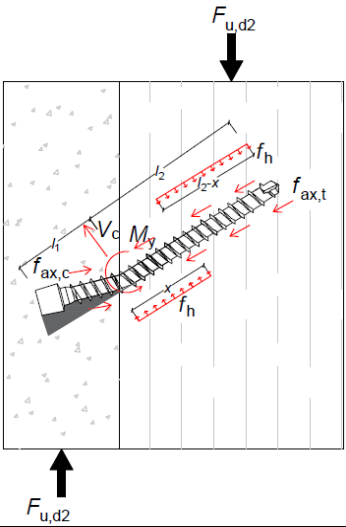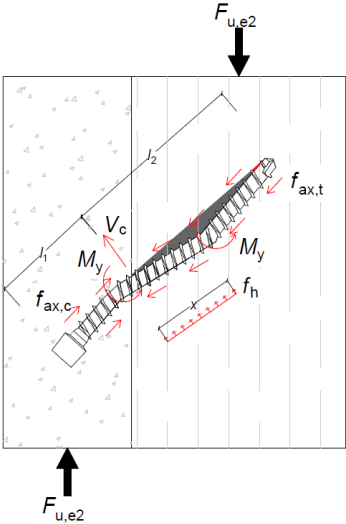
$$f_c = 3f_{c,k} \tag{8}$$

$$F_{failure} = \min\left(F_{u,a}, F_{u,b}, F_{u,c}, F_{u,d1}, F_{u,d2a}, F_{u,e1}, F_{u,e2}, F_{u,f}\right) \tag{9}$$

Table 1 Failure modes to take into account in the determination of the load capacity of shear connection

Failure mode	Scheme	Equation derivation
Case a Embedment strength of the concrete is reached		$F_{u,a} = F_{ax}\cos\alpha + f_c d l_1 \sin\alpha$
Case b Embedment strength of the timber is reached		$F_{u,b} = F_{ax}\cos\alpha + f_h d l_2 \sin\alpha$
Case c Embedment strength of the timber and concrete is reached with rotation of the connector without development of a plastic hinge		$F_{u,c}$ $= F_{ax}\left(\mu\sin\alpha + \cos\alpha\right) + \dfrac{f_c d l_1}{1+\beta}\,(1$ $- \mu\cot\alpha)\left[\sqrt{\beta + 2\beta^2\left[1 + \dfrac{l_2}{l_1} + \left(\dfrac{l_2}{l_1}\right)^2\right] + \beta^3\left(\dfrac{l_2}{l_1}\right)^2}\right.$ $\left. - \beta\left(1 + \dfrac{l_2}{l_1}\right)\right]$

Case d1 Development of a plastic hinge in the connector in the timber layer and embedment strength of the timber and concrete are reached		$$F_{\mathrm{u},d1}$$ $$= F_{\mathrm{ax}}(\mu \sin \alpha + \cos \alpha) + (1$$ $$- \mu \cot \alpha)\frac{f_c d l_1}{2+\beta}\left[\sqrt{2\beta(1+\beta) + \frac{4\beta(2+\beta)M_y}{f_c d l_1^2}} - \beta\right]$$
Case e1 Development of a plastic hinge in the connector in the concrete layer and the embedment strength of the concrete and timber is reached		$$F_{\mathrm{u},e1}$$ $$= F_{\mathrm{ax}}(\mu \sin \alpha + \cos \alpha) + (1$$ $$- \mu \cot \alpha)\frac{f_c d l_2}{1+2\beta}\left[\sqrt{2\beta^2(1+\beta) + \frac{4\beta(1+2\beta)M_y}{f_c d l_2^2}}\right.$$ $$\left. - \beta\right]$$
Case f Development of two plastic hinges in the connector: one in the timber layer and one in the concrete layer and embedment strength of both materials is reached		$$F_{\mathrm{u},f} = F_{\mathrm{ax}}(\mu \sin \alpha + \cos \alpha) + (1$$ $$- \mu \cot \alpha)\sqrt{\frac{2\beta}{1+\beta}}\sqrt{2M_y d f_c}$$

Case d2 Development of a plastic hinge in the connector at the timber-concrete interface and the embedment strength of the timber is reached		$$F_{u,d2} = F_{ax}(\mu \sin\alpha + \cos\alpha) + (1 - \mu\cot\alpha)f_h dl_2\left[\sqrt{2}\sqrt{\frac{2M_y}{f_h dl_2^2} + 1} - 1\right]$$
Case e2 Development of two plastic hinges in the connector at the timber layer and the embedment strength of the timber is reached		$$F_{u,e2} = F_{ax}(\mu \sin\alpha + \cos\alpha) + 2(1 - \mu\cot\alpha)\sqrt{M_y d f_h}$$

2.3. Ductility

The level of ductility a shear connection presents determines its capacity to redistribute the shear force within the different shear connectors along the composite member. Accordingly, the distribution of shear connectors can be varied from non-uniform to uniform (which is preferable in practice). Consequently, determining the ductility is an important task when characterizing a shear connection.

The use of steel fasteners is preferred in TCC due to their reliability and ductile behaviour. The comparison of force-slip curves of various types of connectors demonstrates that screws fall into a category in which optimized load carrying capacity and ductility are obtained [8].

In the background document for the Technical Specification for TCC [27], ductility (D) is recommended to be determined through the method given in the EN 12512 [28], as expressed in Eq. (10). In this formula, v_u, represents the slip at ultimate load and v_y represents the connection yield slip, as illustrated in Figure 1. According to the EN 12512 [28], the ultimate slip (v_u) can be determined using three different approaches: a) slip corresponding to the failure load (F_{max}), b) slip corresponding at 80% of the failure load (after maximum load is attained) or c) slip of 30 mm. Determining the yield slip is,

however, more complex since there is no clearly defined yield plateau, and different approaches can be used as summarised by Jorissen and Fragiacomo [29]. In this study the approaches given by the EN 12512 is used [28].

According to the EN 12512, the yield slip is determined by the intersection of two lines as illustrated in Figure 1. The first line, is the slope between the load and slip corresponding to the 40% and 10% of the failure load as given in Eq. (11) and represents the secant stiffness of the connection in the elastic range. The second line is drawn with a slope that is one sixth of the previous and intersects the force-slip curve at F_{max}, as expressed in Eq. (12). The yield slip value is then obtained at the intersection of these two lines.

$$D = \frac{V_u}{V_y} \tag{10}$$

$$\tan \alpha = \frac{0.4F_{max} - 0.1F_{max}}{v_{0.4} - v_{0.1}} \tag{11}$$

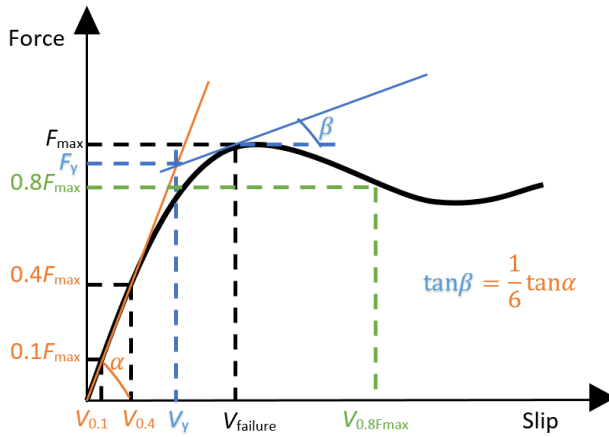$$\tan \beta = \frac{\tan \alpha}{6} \tag{12}$$

Figure 1 Procedure to define ultimate and yield slip values based on EN 12512 [28]

3. Experimental campaign
3.1. Test specimens, layout and monitoring

Short-term push-out tests were performed to characterise the mechanical behaviour of the shear connection between timber and low strength lightweight concrete using screw connectors. The test specimens were made of a timber member with two concrete slabs, one on each side (symmetric configuration). They consist of: i) glued laminated timber with strength class GL24h according to EN 14080 [30]; ii) screw connectors ASSY plus VG from Wurth [25]; iii) lightweight concrete with Argex® aggregate of strength class LC 12/13 according to the EN 1992-1-1 [31]. In Figure 2 the two main types of specimens according to the position of the screw connector are illustrated. The out-of-plane dimensions of the different parts are the following: i) timber, 90 mm; ii) concrete slab, 190 mm. To observe the effects of different screw diameter, screw length and angle to the grain (90° and 45°), three different screws were used: M8x160, M8x200, and M10x200. The complete test programme and testing variables are summarised in Table 2. Each screw is chosen in a way that they can be related to each other either by their diameter or length, in order to isolate the effect of each testing variable. The label of the test specimens (ID) consist on the following: screw - screw diameter - screw length - screw

drilling angle - number of specimens. The screws are threaded throughout the entire length. The screw spacing is respected as recommended in both the ETA document [25] and EN 1995-1-1 [6]. Overlapping of screws is avoided following the recommended spacing given in the EN 1995-1-1 [6]. Each side is shifted 10 mm, up or down. Properties of the screws can be found in the ETA document [25]. In the out of plane direction of the sketch given in Figure 2, screws are aligned at the centreline of the timber. The penetration length of the screw in concrete is chosen to be 50 mm to satisfy the screw ETA requirements [25]. Material properties and connector properties can be found in ETA – 11/0029 [25].

In what concerns the LWC, compression tests on cubes were performed according to EN 12390 - 3 to determine its basic properties [32]. The obtained 28-day compressive strength and density class was 14.5 MPa and D1.4, respectively. The Young's modulus (10934 MPa) was determined according to EN 1992-1-1 [31].
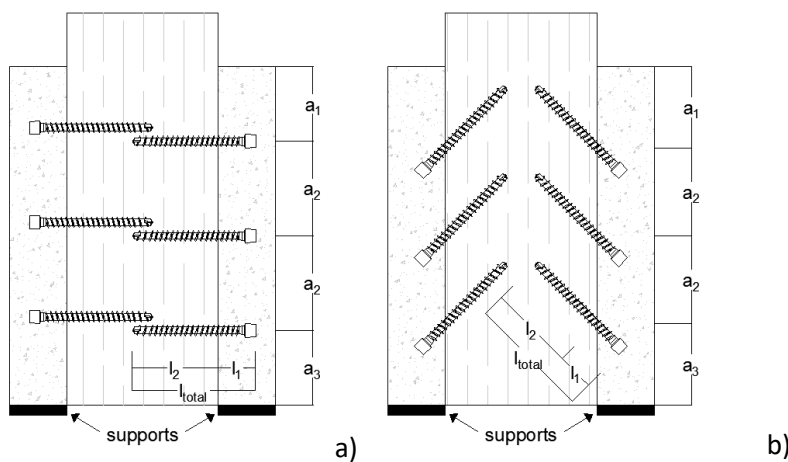

Figure 2 Cross-section of the test specimens (a) for 90°angle configuration (b) for 45°angle configuration

Table 2 Test specimen dimensions

ID	d	l_{total}	α	l_2	l_1	a_1	a_2	a_3	number of tests
S-M8-160-45	8	160	45	110	50	120	130	120	3
S-M8-200-45	8	200	45	150	50	120	130	120	3
S-M10-200-45	10	200	45	150	50	110	130	130	3
S-M8-160-90	8	160	90	110	50	110	130	130	3
S-M8-200-90	8	200	90	150	50	110	130	130	3
S-M10-200-90	10	200	90	150	50	135	140	105	3

The experimental set-up is illustrated in Figure 3 and consists on the application of a push-out load on the timber member up to failure. The test specimen is supported at the opposite side (to the loading) within the full surface of the concrete slabs. The monitoring of the tests was accomplished using a load cell and LVDTs (Linear Variable Differential Transformer). The first measured the total force applied to the specimen by the hydraulic jack. An LVDT was placed at the bottom of the test specimen, as illustrated in Figure 3. The specimen is not restrained in the horizontal direction to avoid a limitation on horizontal separation.
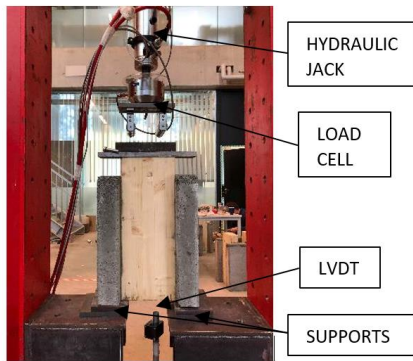
Figure 3 Experimental set-up

3.2. Tests results

In Figure 4 and Figure 5, the load-slip curves for the configurations with 90° and with 45° are shown, respectively. The slip is measured using LVDT, which measures the relative displacement between the timber and the concrete in the load direction. The curves are not limited to a specific slip value in order to observe the behaviour of the screws after a maximum load capacity was achieved. From these figures, it is possible to observe a uniform trend in the elastic range within each case.

Table 3 and Table 4 summarise the main parameters allowing the characterisation of the shear connection for screw connectors installed at 90° and 45° angle to the timber grain, respectively. The slip modulus given in these tables are for both connections (left-hand side and right-hand side). The ultimate deformation, v_u, was determined using the slip corresponding to 80% of the maximum load after failure, in correspondence with criterion b) described in section 2.3. The type of mode of failure is also included. It can be observed that the tests for the shear connection with screws installed at 45° have smaller deviations when compared to the other configuration. A more detailed analysis of these results is given later in section 4.
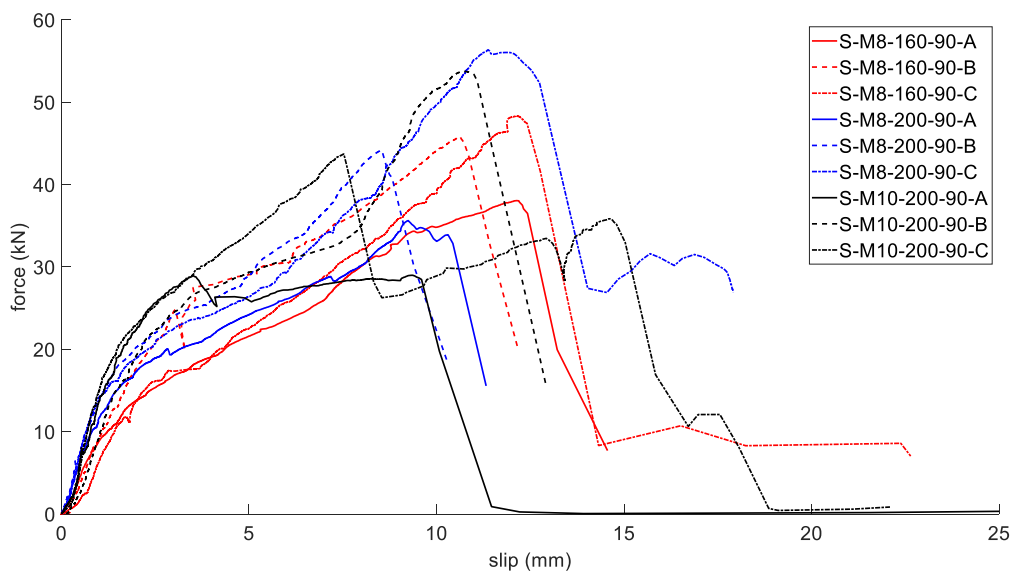

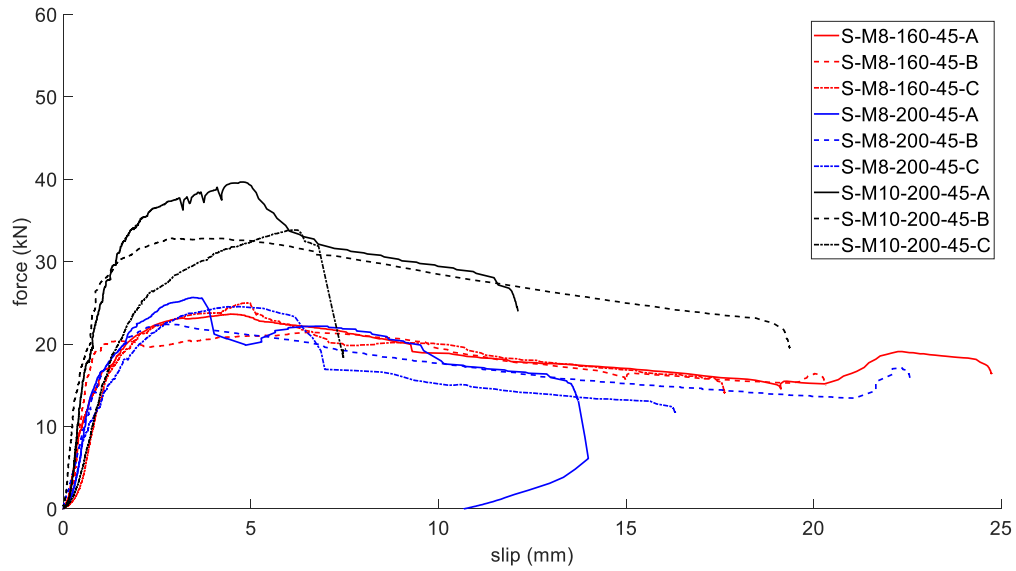*Figure 4 Force-slip curve for the 90° angle configuration*

Figure 5 Force-slip curve for the 45° angle configuration

Table 3 Experimental results for 90°angle configuration

ID	*K*ser (tan(*α*))	*F*max (kN)	*v*u (mm) - EN 12512	Observed failure
S-M8-160-90-A	5.71	38.05	12.72	Longitudinal splitting of concrete (Figure 6)
S-M8-160-90-B	9.11	45.83	11.22	
S-M8-160-90-C	5.72	48.30	12.91	
Mean	6.85	44.06	12.28	
Standard deviation	1.96	5.35	0.93	
COV (%)	28.63	12.14	7.54	
S-M8-200-90-A	10.07	35.63	10.66	Longitudinal splitting of concrete (Figure 6)
S-M8-200-90-B	11.60	44.18	9.11	
S-M8-200-90-C	6.45	56.36	13.12	
Mean	9.37	45.39	10.96	
Standard deviation	2.64	10.42	2.02	
COV (%)	28.22	22.95	18.44	
S-M10-200-90-A	15.93	28.99	9.89	Longitudinal splitting of concrete (Figure 6)
S-M10-200-90-B	10.29	53.75	11.56	
S-M10-200-90-C	17.08	43.72	7.98	
Mean	14.43	42.15	9.81	
Standard deviation	3.63	12.45	1.79	
COV (%)	25.18	29.54	18.26	

Table 4 Experimental results for 45°angle configuration

ID	Kser (tan(α))	Fmax (kN)	vu (mm) - EN 12512	Observed failure
S-M8-160-45-A	27.40	23.64	9.89	Local concrete crushing combined with plastic deformation of dowels (Figure 7)
S-M8-160-45-B	39.12	21.41	13.52	
S-M8-160-45-C	20.26	24.98	7.46	
Mean	28.93	23.34	10.29	
Standard deviation	9.52	1.80	3.05	
COV (%)	32.92	7.71	29.64	
S-M8-200-45-A	24.61	25.66	4.46	Local concrete crushing combined with plastic deformation of dowels (Figure 7)
S-M8-200-45-B	18.74	22.39	9.52	
S-M8-200-45-C	19.03	24.54	6.80	
Mean	20.79	24.20	6.93	
Standard deviation	3.31	1.66	2.53	
COV (%)	15.91	6.86	36.56	
S-M10-200-45-A	39.88	39.67	7.12	Local concrete crushing combined with plastic deformation of dowels (Figure 7)
S-M10-200-45-B	51.76	32.83	13.07	
S-M10-200-45-C	9.98	33.84	8.39	
Mean	33.87	35.45	9.53	
Standard deviation	21.53	3.69	3.13	
COV (%)	63.55	10.41	32.89	

- **Screw connectors at 90° angle to the grain**

For the 90°configuration (Figure 4), the force increases until the maximum load, with a "limit" of elastic capacity followed by a "hardening zone". Once this point is reached, there is a significant loss of capacity, since the load drops approximately by 50%. After this point, significant eccentricities take place leading to the development of out-of-plane bending and therefore the tests no longer represent the mechanical behaviour of the shear connection. Consequently, it can be observed that the deformation capacity after the maximum load is very small, and therefore the ductility appears to be limited. For some test specimens a post-failure strength is still noticed however, this results from the modification on the load transfer mechanism due to eccentricities referred before. Furthermore, the load-slip curves show a similar pattern demonstrating the consistency of the test results.

For the test specimens with screws installed at 90° angle to the grain direction, the most observed failure is failure in the concrete, as shown in Figure 6. It is observed that a common crack is formed connecting all screws until the concrete is broken in two or more pieces. This crack initially developed at the location of the screws (local pressure between the screw and concrete) and propagated towards the edge. This failure pattern may explain the obtained force-slip curve. Until the local bearing capacity of the concrete is reached, the response is approximately linear. Then, a loss of stiffness is significantly observed but with increasing strength ("hardening" zone). Finally, the ultimate deformation, in this case corresponding to the maximum load capacity, is achieved with overturning of the specimens or completeness of the crack. Once the shear connection fails in one side of test specimen (complete

crack formation), there is a loss of equilibrium. The resulting asymmetry creates eccentricities and consequently, out-of-plane forces such as rotation in the system.

Figure 6 Failure of specimens with screws installed at 90 degrees to the timber grain

▪ **Screws at 45° angle to the grain**

The behaviour of the connections with screws installed at 45° (Figure 5) differs from the previous configuration. For these connections, the response only shows nonlinearity in the range near the maximum load. Then, contrary to the connections with screws installed at 90°, for the majority of cases the loss of load capacity is less significant and followed by a significant deformation capacity. This allows to conclude that a more ductile response is obtained and indicates that plastic deformations occur in the screw connector.

In case of inclined screws, the failure mode was different, as shown in Figure 7. In these test specimens, though failure remained in the concrete side, it occurred locally, no common crack connecting the screws was formed. The bearing resistance of the concrete component was reached with loss of the withdrawal capacity, as can be seen in Figure 7-b) through the gap between concrete and timber. In addition, plastic deformation of the screws was also achieved. This justifies the maximum load attained before ultimate deformation which for most of the test specimens was followed by some deformation capacity without significant loss of load capacity (see Figure 5). In these tests, the following combination of phenomena can be identified: i) failure of concrete Figure 7(a), ii) withdrawal of the screws Figure 7(b), iii) no common cracks were observed connecting all screws Figure 7(c) and iv) yielding of the screw Figure 7(d). These observations are consistent with the force-slip curve presented in Figure 5.
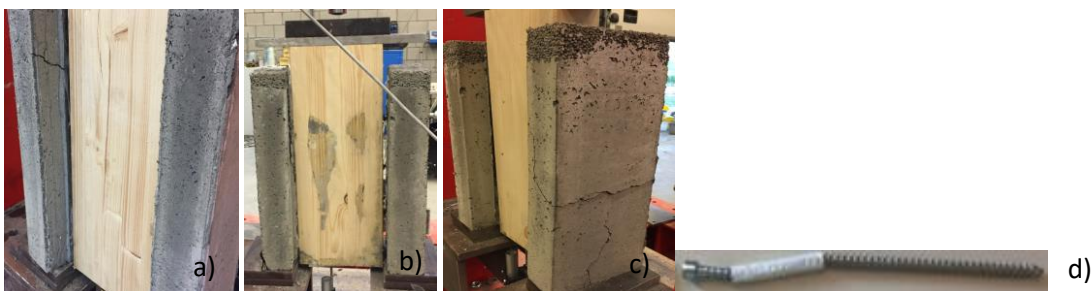

Figure 7 Failure of specimens with screws installed at 45 degrees to the timber grain (from left to right) (a) Concrete failure (b) timber withdrawal failure (c) crack pattern of the loaded specimen (d) plastic hinge formation in a failed screw

4. Discussion of results and new proposals
4.1. Comparison between testing variables

In this subsection, the effect of each testing variable is discussed. The analysis is based on mean values of the experimental tests given in Table 5. This table summarizes the results given in Table 3 and Table 4. The slip (v_y) corresponds to the limit of elastic deformation calculated according to EN 12512 as described in section 2.3 [28].

Table 5 Mean values of the experimental results based on EN 12512 [28]

ID	K_{ser} (tan(α))	F_{max} (kN)	v_u (mm)	v_y (mm)	D
S-M8-160-90	6.85	44.06	12.28	5.27	2.34
S-M8-200-90	9.37	45.39	10.96	2.12	5.66
S-M10-200-90	14.43	42.15	8.80	1.29	8.06
S-M8-160-45	28.93	23.34	10.29	0.75	13.58
S-M8-200-45	20.79	24.20	6.93	1.05	6.54
S-M10-200-45	33.87	35.45	9.53	1.06	8.90

- **Effect of embedment length on timber layer**

The connector embedment length in the timber layer was varied while it was kept constant in the concrete layer (50 mm). The effect of this parameter can be analysed comparing the test specimens with embedment lengths of 160 mm and 200 mm, for both configurations with the connector applied at 90° and 45° angle to the grain.

According to EN 1995-1-1 [6], the embedment length of a connector does not affect the stiffness. Using the specimens with lowest embedment depth (160 mm) as a reference, it is possible to observe variations on the initial slip modulus (K_{ser}), approximately 32% of increase and 17% of decrease, for specimens installed at 90° and 45°, respectively. These results have to be read with care because the determination of the slip modulus is dependent on the applied method. In this case the secant slip modulus (K_{ser}) at coordinates 40% and 10% of maximum load is used. As it can be observed in Figure 4, because the force-deformation curve presents a limit of elasticity significantly smaller than the maximum load capacity, the slip modulus is considerably influenced by the behaviour in the post-elastic range which is more variable for test specimens with screws installed at 90°.

In terms of load carrying capacity, a comparison between the test specimens confirms the conclusions drawn in chapter 3. For a screw installation angle of 90° the maximum load capacity (F_{max}) is governed by the concrete, and in the case of the specimens with 45°, combined with plastic deformations on the connector. Consequently, the embedment depth has an insignificant impact on the load capacity. The variation on the embedment length resulted in an increase of approximately 3% for both types of specimens.

For the test specimens installed at 90°, an increased embedment length leads to an increase in ductility ratio. For the test specimens with screws installed at 45°, a decrease in ductility ratio is observed. This is mainly due to a significant decrease of the ultimate slip (v_u).

- **Effect of screw angle**

The variation of the screw angle allows the comparison of three pairs of specimens where all other variables are equal.

Again, in EN 1995-1-1 the angle between the connector and the timber grain is not taken into account for the stiffness [6]. The results in this study shows that varying the angle from 90º to 45º results in a significant increase of the slip modulus (K_{ser}), above 100%, in all cases. This increase is in agreement with literature for the use of two materials with similar Young's modulus [14]. Part of the observed difference is due to the determination of a secant stiffness using the maximum load capacity as a reference (40% and 10% of F_{max}). This observation is well illustrated when comparing the force-slip curves given in Figure 4 and Figure 5.

In what concerns the load-carrying capacity, the variation of the screw angle from 90º to 45º resulted in a decrease of the load carrying capacity for all cases. The decrease is approximately 47% and 17%, for specimens with a M8 and M10 connector, respectively. The test results confirm the expected response: inclined screws in shear-compression are less efficient than screws installed at 90º because the friction component is removed.

In terms of ductility, changing the angle from 90º to 45º lead to an increase of the ductility ratio. Figure 8 illustrates the limit of elastic slip (v_y) and ultimate slip (v_u) which corresponds to the 80% of the failure load (maximum load) after the failure. Due to brittle failure of the concrete in the 90º angle, the difference between two slip values are similar and a less ductile behaviour is observed. For the 45º angle, due to the plastic deformation in the screws, more ductile behaviour is obtained. Furthermore, Figure 8 highlights the significant deformation capacity of the connection, as after reaching the ultimate slip (v_u), the load capacity, though decreasing, remains significant.
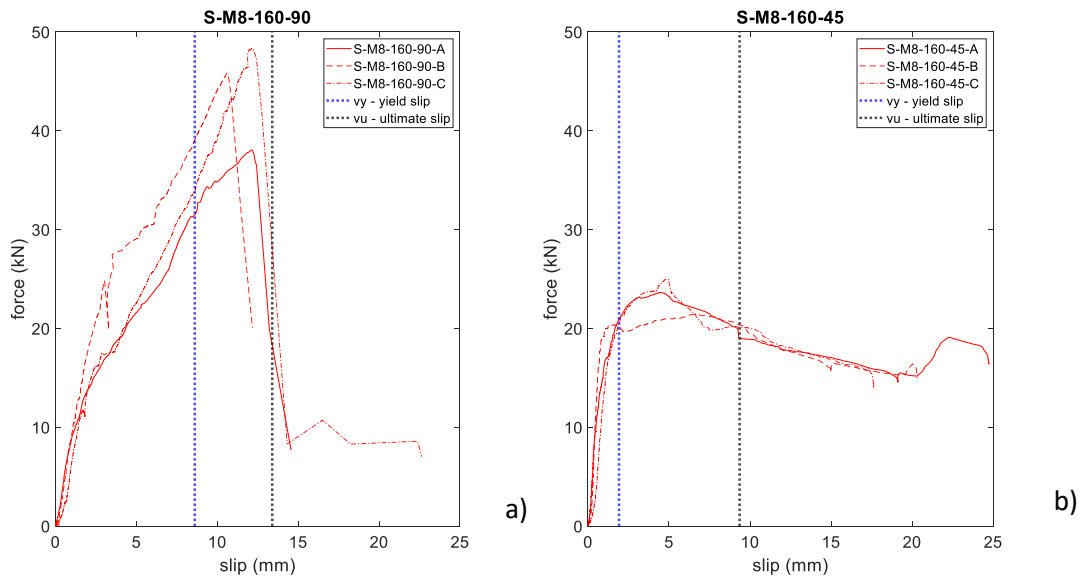

Figure 8 Yield slip and ultimate slip presentation on S-M8-160 (a) for 90°angle (b) for 45°angle

- **Effect of screw diameter**

According to the EN 1995-1-1 [6], the screw diameter should affect both slip modulus (K_{ser}) and load carrying capacity (F_{max}). In the performed tests, the effect of screw diameter is analysed comparing the test specimens M8-200 and M10-200, for each angle separately.

For both, 90° and 45° installation angle, the slip modulus increases with the increase of screw diameter, the observed increase is above 14%. This confirms the influence of the screw diameter in this parameter.

In what concerns the load carrying capacity, the results are very distinct according to the angle of installation of the screw connector. For 90° there is minor variation, while for 45° a significant increase is observed, about 32%. This reflects the participation of the bending strength of the screw connector on the load capacity of the shear connection, as already concluded above. It is clear that the load capacity for specimens installed at 90° is mainly governed by the concrete with less participation of the screw connector.

The ductility is also affected by the diameter of the screw. In both situations, 90° and 45° installation, an increase is observed. For a 90° angle, the drop down on the force-slip curves is governed by the crack propagation in the concrete. This increase can be justified by a better distribution of stresses in the concrete due to the bigger screw diameter for test specimens using a M10 screw.

4.2. Comparison between experimental tests and analytical approach
4.2.1. Stiffness

In Table 6 and Table 7 the values are given obtained in the experimental tests and through the analytical models, respectively. As exposed in chapter 2, the determination of the slip modulus can follow two analytical approaches, either using Eq. (1) or Eq. (2). In order to evaluate the quality of the approximation, the difference between experimental results and analytical predictions was computed (Δ) in terms of percentage.

For the perpendicular case (Table 6), it was expected to obtain a good agreement between the code requirement, EN 1995-1-1 [6], and the experimental results. However, the use of Eq. (2) leads to a minimum of 86% percentage difference by overestimation. Use of Eq. (1) (which results in half of the value obtained with Eq. (2)) was much better and leads to a smaller difference with the experimental results. It also should be noted that the secant stiffness is taken into consideration which is one of the reasons of the obtained difference. Nevertheless, the use of the timber-to-timber slip modulus (Eq. (1)), is more accurate. As proposed by the authors, this indicates that if two different materials have a similar Young's modulus, the slip modulus should not be doubled as proposed in the code.

Table 6 Comparison of experimental results for perpendicular application with analytical approach (K_{ser} in kN/mm)

ID	Experimental (EN 12512)	Analytical (EN 1995-1-1)			
	K_{ser} (tan(α))	K_{ser} Eq. (1)	Δ (%)	K_{ser} Eq. (2)	Δ (%)
S-M8-160-90	6.85	10.84	-58.33	21.68	-216.67
S-M8-200-90	9.37	10.84	-15.64	21.68	-131.27
S-M10-200-90	14.43	13.44	6.89	26.88	-86.23

The results in Table 7 show the use of Eq. (1) and Eq. (2) and comparison with the experimental results for the 45° configuration. This analysis shows that the use of Eq. (1), which represents the stiffness prediction for timber-to-timber connections, is not suitable for shear-compression. Comparing with the approach defined in Eq. (2), the experimental results are in good agreement however, the increased stiffness is due to the contribution of the connector axial stiffness which is activated from

the beginning of the loading. These results show that the use of shear-compression loaded screws does not necessarily have a negative effect on the composite action of the TCC system.

Table 7 Comparison of experimental results for inclined application with analytical approach (K_{ser} in kN/mm)

ID	Experimental (EN 12512)	Analytical (EN 1995-1-1)			
	K_{ser} (tan(α))	K_{ser} Eq. (1)	Δ (%)	K_{ser} Eq. (2)	Δ (%)
S-M8-160-45	28.93	10.84	62.52	21.68	25.05
S-M8-200-45	20.79	10.84	47.86	21.68	-4.28
S-M10-200-45	33.87	13.44	60.32	26.88	20.65

4.2.2. Load carrying capacity

The experimental results are compared with the predictions given in section 2.2 for the load-carrying capacity of the specimens. The expected failure load is determined by the minimum of the predicted loads, as expressed in Eq. (9).

- **90° angle configuration**

In Table 8 the load capacity is given for each mode of failure identified in Table 1. Both the load capacity without and with rope effect are given. At the first phase of loading, the capacity of the member is based on Johansen's model (F_u) given in Section 2.2. Once this load is achieved, with transition to post-elastic stage, rotations in the screws start occurring, which activate the axial forces in the screws contributing to the load capacity, as described in section 2.2. This component (the rope effect) is then added to the load capacity based on Johansen's model and determined as defined in the code [6]. In Figure 9, the force-slip curves and expected failure loads are plotted for each configuration. For the latter, both values, without and with rope effect, are represented. It is interesting to notice that the values without the rope effect are near to what could be considered as an elastic limit. As it can be observed, a nonlinear relation begins after the first horizontal line in the charts. Then, because the rope effect develops, the load capacity of the connection is increased, however, with a significant loss in stiffness because of screw rotation, with or without yielding, depending on the test specimen, as shown in Figure 10.

When the expected load capacity is compared with the experimental results, the model is close for M8 and not so much for M10 (see Table 8). The reason for the latter is due to a longitudinal splitting of the concrete, as presented in Figure 6, which leads to a similar experimental load capacity independently of the screw diameter. This mode of failure was not covered in section 2.2 and is due to the concrete strength and dimensions, and does not represent the local connection. Furthermore, the load predictions, and the expected modes of failure, demonstrate a consistency with the experimental observations. According to the values without rope effect, the governing failure mode is mode e_2. With activation of the rope effect, which results from a rotation and possible formation of plastic hinges in the screw, the expected failure modes changed for all specimens. For the latter, mode c is now the governing mode of failure. The final expected mode of failure are consistent with the experimental observations as reported in Figure 10. The screws of test specimens M8x160 (Figure 10-a) and M10x200 (Figure 10-c) do not show significant plastic deformations. This is consistent with mode c, where the activation of the rope effect results of screw rotation. While for test specimens M8x200 (Figure 10-b) the screws present a clear development of two plastic hinges, as preconized by mode f

and e_2). It should be mentioned that the difference between modes f and e_2, is the location of the plastic hinge on the concrete side (see Table 1). From the tests, the location of the plastic hinge on the concrete side is not clear.

Table 8 90°angle calculations units in kN

| Cases	Johansen's resistance F_u (Without F_{ax} (kN))			Rope effect contribution min($F_{ax}/4,F_{yRk}$)			Shear connection resistance With min($F_{ax}/4,F_u$)		
	M8x160	M8x200	M10x200	M8x160	M8x200	M10x200	M8x160	M8x200	M10x200
Case a	11.45	15.62	30.09	0.00	0.00	0.00	11.45	15.62	30.09
Case b	11.96	11.96	14.83	0.00	0.00	0.00	11.96	11.96	14.83
Case c	4.81	6.08	10.73	2.61	3.56	4.05	**7.42**	9.64	**14.78**
Case d	4.46	5.95	10.89	2.61	3.56	4.05	14.22	19.04	32.36
Case e	3.84	3.84	5.48	2.61	3.56	4.05	12.59	13.54	18.30
Case f	2.41	2.41	4.15	2.41	2.41	4.05	9.28	**9.28**	15.88
Case d2	5.00	6.66	12.80	2.61	3.56	4.05	15.01	20.07	35.80
Case e2	**1.44**	**1.44**	**2.69**	1.44	1.44	2.69	9.67	9.67	18.01
Min F_u	**1.44**	**1.44**	**2.69**				7.42	9.28	14.78
For 6 screws	**8.66**	**8.66**	**16.12**				44.53	55.65	88.68
Experimental	**44.06**	**45.39**	**42.15**				44.06	45.39	42.15
Difference (%)	**80.35**	**80.92**	**61.74**				-1.06	-22.60	-110.39
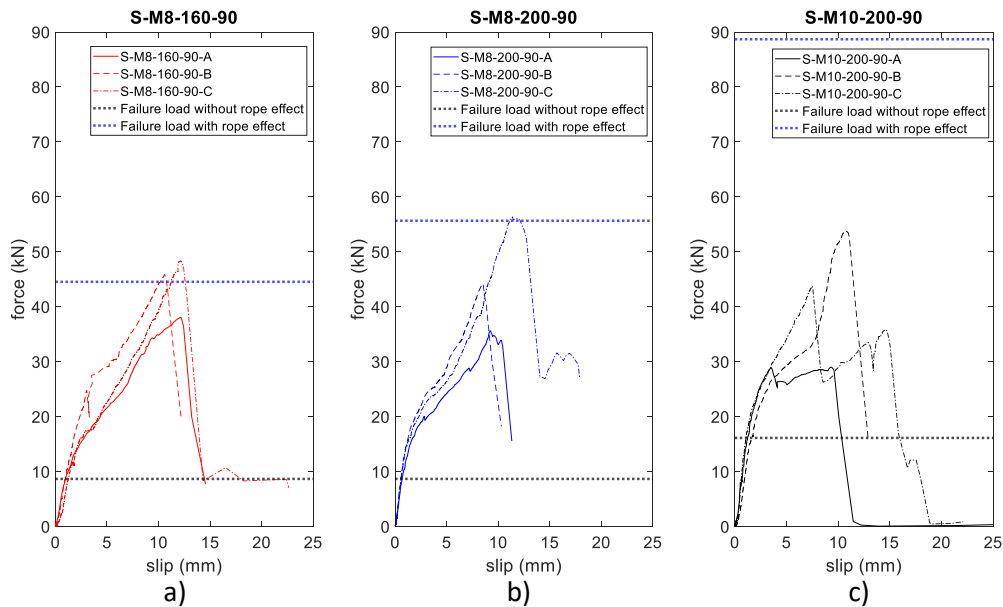
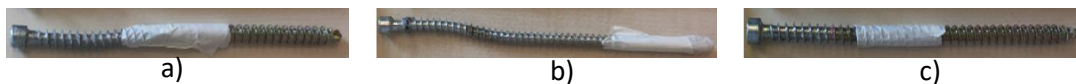*Figure 9 90 degree angle force-slip curves with failure load predictions*

Figure 10(a) M8-160-90-B failed screw (b) M8-200-90-C (c) M10-200-90-B failed screw

▪ **45° angle configuration**

For inclined screws, as discussed in section 2.2, the withdrawal capacity is activated from the beginning of the load while the shear-compression loading implies the loss of the friction component. In Table 9, the load capacity for the possible modes of failure are given. Accordingly, mode *f* is the governing mode of failure. The smallest difference between the experimental tests and the predicted load capacity is still 130%. Figure 11 illustrates the force-slip curve for each configuration along with the expected failure load and highlights the differences. Figure 12 shows the plastic hinges formed in the screws, confirming mode *f*. Based on these results, and based on the clear separation between the two materials, as shown in Figure 7-b), it is clear that the screw withdrawal capacity had a major role in the load capacity of these test specimens. However, as normally assumed in TCC, and also in the approach given in section 2.2, the withdrawal capacity here was not governed by the timber side but by the concrete side. Furthermore, the mechanics of the shear-compression configuration is pushing the two materials apart, resulting in a pull-out of the screw from the concrete layer. Consequently, a local failure mode occurred which limited the withdrawal capacity of the connection. This mode of failure is known as pull-through (common in pull-out of anchorages in concrete) and occurs when the concrete is crushing at the head of the screw. This is in line with the proposal of Jorge et al. [33], which states that the local failure between the screw and concrete can occur.
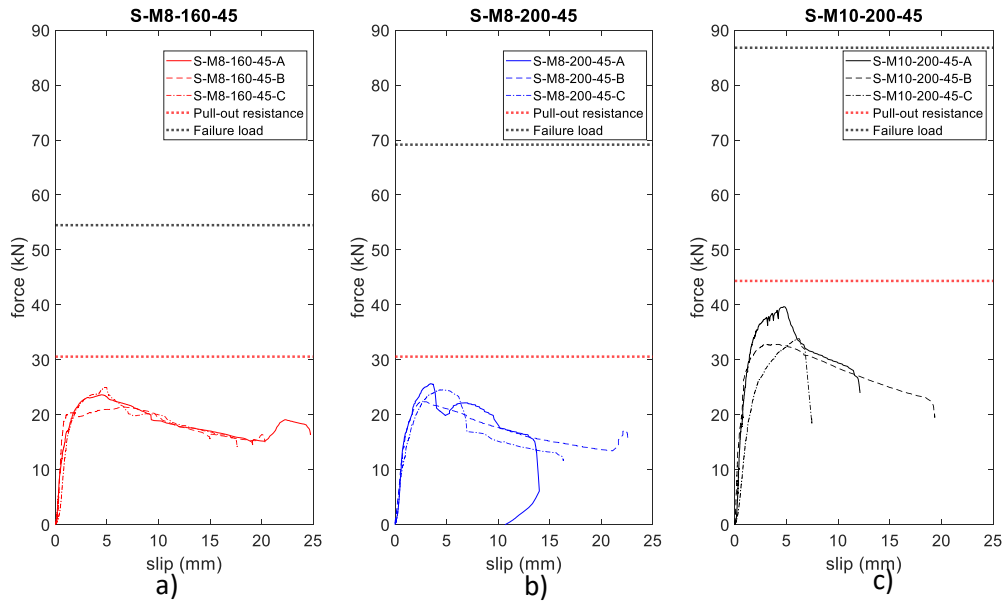

Figure 11 45 degree angle force-slip curves with failure load predictions including pull-out resistance
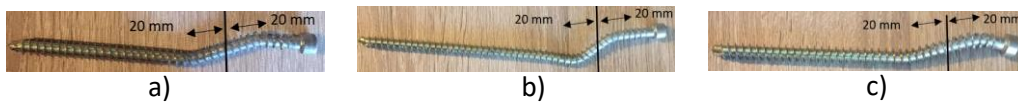

Figure 12 Failed specimens for 45 degree angle configuration (from left to right) (a) gap between the concrete and the timber layer (b) M-8-160-45 failed screw (c) M-8-200-45 failed screw (d) M-10-200-45 failed screw

In Table 9, the load capacity for each mode of failure are re-calculated considering the pull-though resistance ($N_{Rk,p}$) as the withdrawal capacity. The comparison is further highlighted in Figure 11. With the proposed approach, the failure load difference decreased to an average of 30% while keeping the same failure mode, and therefore still consistent with the experimental observations. Nevertheless, an overestimation is still noticed, which may be justified by the fact that Eq. (7) was proposed for a different type of connector. Specific experimental tests are needed to better characterize the pull-through of the screw installed in concrete, and in particular lightweight aggregate concrete. Even

though some concepts are explained in this paper, a detailed numerical analysis can be beneficial as is done in the literature [34].

Table 9 Failure load prediction and comparison of 45° angle calculations with headed fastener characteristic resistance units in kN *(expected failure load and experimental comparisons are highlighted)*

Cases	Johansen's resistance F_u (kN)			Shear connection resistance F_u with $N_{rk,p}$ (kN)		
	M8x160	M8x200	M10x200	M8x160	M8x200	M10x200
Case a	14.81	20.20	31.68	10.83	13.77	24.61
Case b	14.30	16.74	19.81	10.31	10.31	12.74
Case c	11.37	15.10	20.93	7.38	8.67	13.86
Case d	11.13	15.05	21.14	7.14	8.62	14.06
Case e	10.12	12.56	15.26	6.13	6.13	8.19
Case f	**9.08**	**11.53**	**14.47**	**5.10**	**5.10**	**7.39**
Case d2	11.72	15.82	23.21	7.73	9.39	16.14
Case e2	9.60	12.05	15.78	5.61	5.61	8.71
Min F_u	**9.08**	**11.53**	**14.47**	**5.10**	**5.10**	**7.39**
For 6 screws	**54.51**	**69.16**	**86.80**	**30.58**	**30.58**	**44.36**
Experimental	**23.34**	**24.20**	**35.45**	**23.34**	**24.20**	**35.45**
Difference (%)	**-133.54**	**-185.79**	**-144.84**	**-31.02**	**-26.36**	**-25.13**

5. Conclusions

In this paper, the behaviour of shear connections for timber concrete composite beams, using low strength lightweight aggregate concrete and fully threaded screws was studied. This considered the realisation of an experimental programme considering an installation of the screws under angles of 90° and 45° (shear-compression) to the interface between the two materials. The analysis and comparison of the experimental results allowed to withdraw the following conclusions:

- In general, the test specimens with screws installed at 90° presented a higher load capacity than those with screws installed at 45°. However, the force-slip curves show that for the first configuration, a clear loss of stiffness at approximately 50% of the maximum load capacity is noticed.
- In terms of slip modulus, test specimens with inclined screws presented higher values, as expected, given the participation of the axial stiffness of the screw on the global response of the shear connection to the push-out forces.
- The test specimens with inclined screws developed significant plastic deformation which resulted in a more ductile behaviour.

Moreover, an analytical approach to determine the slip modulus and the load capacity of the tested shear connection was proposed to include the use of light-weight concrete. The comparison with the experimental results allowed to assess on the accuracy of the proposal, namely the following was concluded:

- For the slip modulus, considering the concrete deformable, is more realistic than assuming a stiff material for perpendicular application of the screw. For shear-compression loaded screws, steel-to-timber slip modulus prediction is more accurate. This proves that installing

the screws in shear-compression does not lead to a decrease in the composite action. However, for the inclined screws, the increase of stiffness is due to the activation of the axial stiffness of the connector from the beginning of the loading. This is not currently taken into account in the current design approach.

- For the test specimens installed at 90°, the activation of the rope effect has a significant importance on the load capacity. According to these predictions, the contribution of the rope effect is more than 50% of the maximum load capacity.

- For the inclined screw connection, the axial forces that developed play a role from the beginning. These axial forces are taken into account through the withdrawal capacity which is commonly limited by the timber side. However, when shear-compression screws are used and the concrete strength is low, a pull-through failure on the concrete might limit the withdrawal capacity. The tests showed a clear separation between the two materials, indicating that the withdrawal capacity on the concrete side was exceeded, the latter was taken into account improving the predictions. The formula proposed for headed anchors given in the EN 1992-4 was used as an estimation.

Finally, though the use of inclined screws in shear-compression are a practice to be avoided, the present study investigated a situation that can occur. Furthermore, the use of low strength concrete was contemplated. The combination of these two factors resulted in a connection with a relatively low load capacity. On the other hand, the results obtained for the test specimens with screws installed at 90° indicate that the use of low strength lightweight concrete might be an efficient solution for the renovation of timber floors that can benefit of composite behaviour. The installation of the screws in shear-tension or X-installed can provide a more efficient connection between the two materials. Even though only analytical and experimental analyses are conducted within this paper's scope, an extensive numerical analysis campaign is a logical next step in optimising the connection.

References

[1]   M. Van der Linden, "Timber-Concrete Composite Floor Systems," PhD Dissertation, Technical University of Delft, Delft, The Netherlands, 1999.

[2]   L. Jorge, "Timber-concrete structures using lightweight aggregate concrete **/** Estruturas mistas madeira-betão com a utilização de betões de agregados leves [In Portuguese] " Ph. D., University of Coimbra, Coimbra, Portugal, 2005.

[3]   S. Carvalho, T. Panzera, A. Christoforo, J. Fiorelli, F. Lahr, and R. Freire, "Epoxy mortar timber beam upgrading," *International Wood Products Journal,* 2017.

[4]   T. Zahra and M. Dhanasekar, "A generalised damage model for masonry under compression," *International Journal of Damage Mechanics,* Article vol. 25, no. 5, pp. 629-660, JUL 2016 2016.

[5]   L. F. Jorge, J. Schanzlin, S. Lopes, H. Cruz, and U. Kuhlmann, "Time-dependent behaviour of timber lightweight concrete composite floors," (in English), *Engineering Structures,* Article vol. 32, no. 12, pp. 3966-3973, DEC 2010 2010.

[6]   *EN 1995-1-1 - Design of timber structures - Part 1-1: General rules and rules for buildings,* E. C. f. Standardization, 2004.

[7]   *EN 1995-2 - Design of timber structures - Part 2: Bridges,* E. C. f. Standardization, 2004.

[8]   A. Dias, "Mechanical behaviour of timber-concrete joints," PhD, TU Delft, Delft, Netherlands, 2005.

[9]   E. Lukaszewska, "Development of Prefabricated Timber-Concrete Composite Floors," PhD, Department of Civil, Mining and Environmental Engineering, Lulea University of Technology, Sweden, 2009.

[10]   M. Fragiacomo, C. Amadio, and L. Macorini, "Short- and long-term performance of the "Tecnaria" stud connector for timber-concrete composite beams," (in English), *Materials and Structures,* Article vol. 40, no. 10, pp. 1013-1026, DEC 2007 2007.

[11]   COST, *Design of timber-concrete composite structures - A state-of-the-art report by COST Action FP1402 / WG 4*. Shaker Verlag Aachen, 2018.

[12]   COST, C. Sandhaas, J. Munch-Andersen, and P. Dietsch, Eds. *Design of Connections in Timber Structures*. 2018.

[13]   L. Marchi, R. Scotta, and L. Pozza, "Experimental and theoretical evaluation of TCC connections with inclined self-tapping screws," (in English), *Materials and Structures,* Article vol. 50, no. 3, JUN 2017 2017, Art. no. ARTN 180.

[14]   R. Tomasi, A. Crosatti, and M. Piazza, "Theoretical and experimental analysis of timber-to-timber joints connected with inclined screws," (in English), *Construction and Building Materials,* Article vol. 24, no. 9, pp. 1560-1571, SEP 2010 2010.

[15]   H. Blass and I. Bejtka, "Screws with continuous threads in timber connections," presented at the RILEM, 2001.

[16]   I. Bejtka and H. Blass, "Joints with inclined screws," in *CIB, Working Commission W18 - Timber structure*, Kyoto, Japan, 2002.

[17]   A. Kevarinmaki, "Joints with inclined screws," in *CIB, Working Commission W18 - Timber structure*, Kyoto, Japan, 2002.

[18]   H. Du, X. Hu, Z. Xie, and H. Wang, "Study on shear behavior of inclined cross lag screws for glulam-concrete composite beams," *Construction and Building Materials,* 2019.

[19]   H. Du, X. Hu, Y. Jiang, C. Wei, and W. Hong, "Load-carrying Capacity of Self-tapping Lag Screws for Glulam-lightweight Concrete Composite Beams," (in English), *Bioresources,* Article vol. 14, no. 1, pp. 166-179, 2019 2019.

[20]   A. Dias, F. Fragiacomo, R. Harris, P. Kuklic, V. Rajicic, and J. Schanzlin, "Technical Specification – Final Draft - Eurocode 5: Design of Timber Structures - Part 1-3: Structural design of timber concrete composite structures – Final Draft / Project Team CEN/TC 250- SC5.T2," 2019.

[21]   K. Johansen, "Theory of timber connections," *International association of bridge and structural engineering,* vol. 9, pp. 249-262, 1949.

[22]   *EN 1992-2 Design of concrete structures - Part 2: Concrete bridges - Design and detailing rules,* E. C. f. Standardization, 2004.

[23]   J. Porteous and A. Kermani, *Structural timber design to Eurocode 5*. Oxford ; Malden, MA: Blackwell Pub., 2007, pp. xii, 542 p.

[24]   S. Kavaliauskas, A. Kazimieras, and B. Valiunas, "Mechanical behaviour of timber-to-concrete connections with inclined screws," *Journal of Civil Engineering and Management,* vol. 13, no. 3, pp. 193-199, 2007.

[25]   ETA-13/0029, "Self-tapping screws for use in wood-concrete slab kits," ed. ETA-Denmark A/S, 2017.

[26]   *EN 1992-4 Design of concrete structures - Part 4: Design of fastenings for use in concrete*, 2018.

[27]   A. Dias, F. Fragiacomo, R. Harris, P. Kuklic, V. Rajicic, and J. Schanzlin, "Technical Specification – Background Document - Eurocode 5: Design of Timber Structures; Structural design of timber concrete composite structures – common rules for buildings / Project Team CEN/TC 250- SC5.T2," 2019.

[28]   *EN 12512 - Timber structures - Test methods - Cyclic testing of joints made with mechanical fasteners*, 2002.

[29]   A. Jorissen and M. Fragiacomo, "General notes on ductility in timber structures," *Engineering Structures,* Article vol. 33, no. 11, pp. 2987-2997, 2011.

[30]   *EN 14080 Timber structures—glued laminated timber and glued solid timber—requirements*, 2013.

[31]   *EN 1992-1-1 Design of concrete structures - Part 1-1: General rules and rules for buildings,* E. C. f. Standardization, 2004.

[32]   *EN 12390-3 Testing hardened concrete - Part 3: Compressive strength of test specimens*, 2009.

[33]   L. Jorge, S. Lopes, and H. Cruz, "Experimental research in timber-LWAC composite structures," in *International Symposium on Advanced Timber and Timber-Composite Elements for Buildings*, Florence, Italy, 2004, pp. 97-104.

[34]   C. Bedon and M. Fragiacomo, "Numerical analysis of timber-to-timber joints and composite beams with inclined self-tapping screws," (in English), *Composite Structures,* Article vol. 207, pp. 13-28, JAN 1 2019 2019.